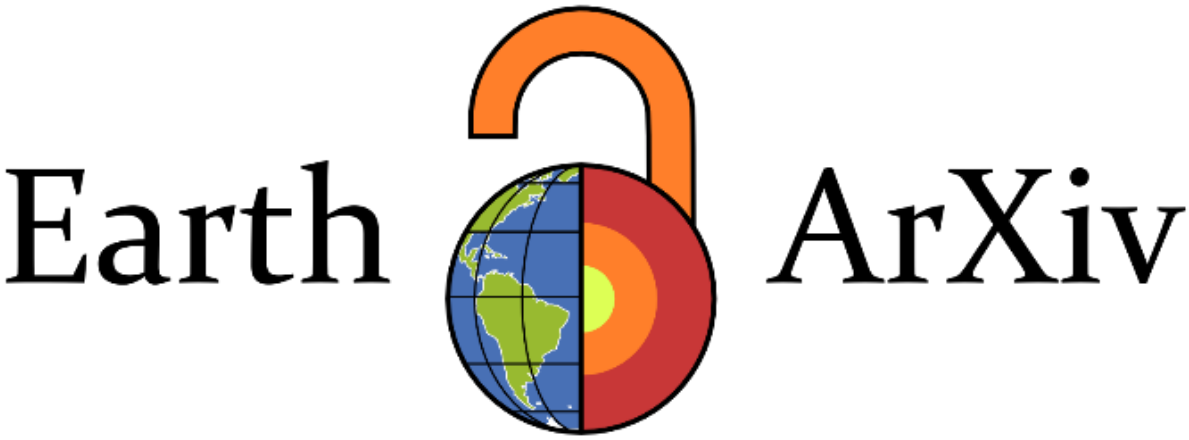

Journal Name

Crossmark

RECEIVED
dd Month yyyy

REVISED
dd Month yyyy

PAPER

How well do global ocean approaches constrain local pCO_2?

Galen McKinley[1,*], Amanda Fay[1], Thea H. Heimdal[1], Lauren Moseley[1,2], Abby Shaum[1]

1 Columbia University and Lamont-Doherty Earth Observatory, New York, NY, USA
2 Carbon to Sea Initiative, Washington, D.C., USA
*Author to whom any correspondence should be addressed.

E-mail: mckinley@ldeo.columbia.edu

Abstract

The ocean absorbs 29% of humanity's annual anthropogenic carbon dioxide (CO_2) emissions, and the future of climate change is strongly dependent on how this sink evolves. Marine Carbon Dioxide Removal (mCDR) approaches to enhance this sink are actively being developed. In the interest of understanding how well state-of-the-art global products and models can help to distinguish mCDR signals from the background ocean carbon sink, we use sparse independent data to quantify their local-scale (1^ox1^o, monthly) errors. Our analysis is for 2000-2023 and uses 5 large regions ("superbiomes") to aggregate sparse data across high-latitude, subtropical and equatorial zones, and we compare to an ensemble of 10 products and 10 models. The observed long-term trend of surface ocean CO_2 due to rising atmospheric CO_2 concentrations is consistently estimated. At the same time, we find substantial biases for the ensemble means: $\pm 5\mu$atm for the products, and ranging from +1 to +15μatm for the models. Across the superbiomes, ensemble-mean unbiased root-mean-square-errors (uRMSEs) are 19-37μatm for the products and 25-56μatm for models. Seasonality is generally well-correlated to the independent data for the products and for the models in the subtropics, but the largest component of uRMSE also lies at this timescale. Deseasonalized variability has smaller uRMSEs and low correlations to independent data. In summary, local-scale, monthly errors in global observation-based products and models for the background ocean carbon sink are more than 1 order of magnitude larger than the local to regional-scale signals likely for open-ocean mCDR ($\sim 1\mu$atm). Reducing local-scale uncertainty in the ocean carbon sink will be critical if these products and models will be part of mCDR monitoring, reporting and verification systems. Improving the representation of seasonality should be a key target for improving both observation-based products and models.

1 Introduction

Given the critical importance of the ocean's uptake of anthropogenic carbon to the future of the global carbon budget and climate change [Canadell et al., 2021, McKinley et al., 2023, Gruber et al., 2023, McKinley, 2026] it is important to understand the accuracy of current estimates of the sink. This sink occurs due to rising atmospheric CO_2 and has taken up 29% of annual anthropogenic CO_2 emissions in the last decade [Friedlingstein et al., 2025a].

If marine Carbon Dioxide Removal (mCDR) approaches will be implemented, the background sink must be quantified as a counterfactual against which additional uptake occuring as a result of the mCDR technology ("additionality") can be evaluated. In this paper and for consistency with the significant literature on this topic, we will refer to the ocean's uptake of anthropogenic carbon that occurs without direct intervention as the *ocean carbon sink*. Engineered approaches will be explicitly identified as mCDR [NASEM, 2022].

When globally-integrated and annually-averaged, the Global Carbon Budget 2025 [Friedlingstein et al., 2025a] estimates that the ocean carbon sink was 3.2 $\pm$ 0.4 PgC yr^{-1} for 2014-2024. This uncertainty has a magnitude of 13% (1σ) of the mean flux for the global integral. Various analyses have shown that when global flux estimates are disaggregated into large regions spanning one or several ocean gyres, differences between the estimates are much larger than 13% for both the long-term mean and seasonality [McKinley et al., 2016, Fay & McKinley, 2021, DeVries et al., 2023, Rodgers et al., 2023, Terhaar et al., 2024]. Not yet reported in the literature

are uncertainties at the smallest scales (1^ox1^o, monthly) of the Global Ocean Biogeochemical Models (GOBMs, or "models") and observation-based products (or "products") used in the Global Carbon Budget. This paper addresses this gap.

Currently, commercial, non-profit and academic research seeks to develop mCDR technologies and the observational and modeling approaches that may be used to quantify the real-world impacts of mCDR deployments [NASEM, 2022]. What will be the baseline estimate of the ocean carbon sink against which perturbations due to mCDR interventions will be measured? Given that the globally-integrated ocean carbon sink is six orders of magnitude larger than all currently-verifiable novel CDR, and that the uncertainty of this sink is also five orders of magnitude larger [Friedlingstein et al., 2025a, Powis et al., 2023], robust estimates of the ocean carbon sink are essential if the very small perturbations to the air-sea fluxes expected from mCDR are to be detected [Wang et al., 2022, Zhou et al., 2024]. This need applies both for the project-scale where a counterfactual for an ocean without mCDR intervention will be needed, as well as for the global scale where net impacts on the atmospheric CO_2 concentration will need to be assessed [Lamarque et al., 2026].

For large oceanic regions, differences across observation-based product and GOBM ensembles of the GCB are large [McKinley et al., 2016, Fay & McKinley, 2021, Terhaar et al., 2024]. Friedlingstein et al. (2025) compare observation-based products to independent data from GLODAP [Olsen et al., 2016, Lauvset et al., 2016, Lauvset et al., 2021] and SOCAT Flag E (quality of ± 10 μatm) [Bakker et al., 2016]. For the globe and for North, Tropical and South regions separated at 30^oN and 30^oS, they find biases are generally within 10μatm and root mean square errors (RMSEs) of 20-50 μatm. The analysis presented here expands these comparisons to include additional independent data, adds GOBMs for equivalent comparisons, and evaluates the dominant timescales of errors for both products and GOBMs. This work improves understanding of the underlying sources of error in ocean carbon sink estimates from the Global Carbon Budget. It is also a first step in understanding the extent to which these global products could be used to quantify the ocean carbon sink that would have occurred in a given location without implementation of mCDR; and thus to be used as the basis for calculations of mCDR additionality.

2 Methods

2.1 Observation-based products and Global Ocean Biogeochemical Models

Here, we evaluate the observation-based products and Global Ocean Biogeochemical Models (GOBMs) (Table 1) used in GCB2024 [Friedlingstein et al., 2025b] for 2000-2023. The Global Carbon Budget (GCB) protocol allows only one submission from each research group. Our Lamont-Doherty Earth Observatory (LDEO) Ocean Carbon research group maintains two products, LDEO-Hybrid Data Physics (LDEO-HPD) [Gloege et al., 2022, Bennington et al., 2022b] and LDEO-Residual [Bennington et al., 2022a, Heimdal et al., 2026], with LDEO-HPD being used in the GCB. Here we include both the LDEO-HPD and LDEO-Residual products. Observation-based products are all trained with SOCAT [Bakker et al., 2016], and thus these data will be excluded from all comparisons to the observation-based products. Per the GCB protocol, observation-based products and GOBMs report fCO_2.

2.2 Independent data

We utilize the merged Global Ocean Data Analysis Project (GLODAP) v2.2023 dataset [Lauvset et al., 2016, Olsen et al., 2016, Lauvset et al., 2021] (downloaded on July 19, 2024). GLODAP contains quality-controlled profiles of various carbonate system parameters with depth, including DIC, Total Alkalinity (TA), as well as temperature and salinity and a variety of other ocean parameters. While fCO_2 is available in the v2.2023 version, it is not quality controlled and there is limited data available for that variable. Therefore, we calculate pCO_2 from surface ($\leq$10m) bottle observations using the CBSYST python package (cbsyst-0.4.10). Inputs to the pCO_2 calculation are GLODAP values for pH, DIC, temperature, salinity, pressure, phosphate, and silicate and a constant average boron concentration of 415.7 μmol/kg. The resulting pCO_2 are converted to fCO_2 according to [Dickson et al., 2007]. Uncertainty is estimated at $\pm 12\mu$atm [Friedlingstein et al., 2025a].

The LDEO Global Ocean Surface Water Partial Pressure of CO_2 Database, developed by Taro Takahashi, compiles surface water pCO_2 measurements to understand the ocean's role in the global carbon cycle [Takahashi et al., 2019]. The 2019 release includes about 14.2 million measurements from 1957 to 2019. The dataset includes only those observations measured using equilibrator-CO_2 analyzer systems, and have been quality-controlled based upon the stability of the system performance, the reliability of calibrations for CO_2 analysis and the internal consistency of data.

Table 1. Observation-based Products (top) and Global Ocean Biogeochemical Models (bottom) in this study.

Product	***Reference***
CMEMS-LSCE-FFNNv2	*Chau et al. 2022*
CSIR-ML6	*Gregor et al. 2019*
Jena-MLS	*Rödenbeck et al. 2022*
JMA-MLR	*Iida et al. 2021*
LDEO-HPD	*Gloege et al. 2022, Bennington et al. 2022b*
NIES-ML3	*Zeng et al. 2022*
OceanSODA-ETHZv2	*Gregor et al. 2024*
UExP-FNN-U	*Watson et al. 2020, Ford et al. 2024*
VLIZ-SOMFFN	*Landschützer et al. 2016, 2020*
LDEO-Residual	*Bennington et al. 2022a*
ACCESS CSIRO	*Law et al. 2017*
CESM-ETHZ	*Doney et al. 2009*
CNRM	*Berthet et al. 2019, Seferian et al. 2019*
FESOM-2.1-REcoM3	*Gurses et al. 2023*
MOM6-COBALT (Princeton)	*Liao et al. 2020*
MPIOM-HAMOCC6	*Lacroix et al. 2021*
MRI-ESM2-3	*Tsujino et al. 2024; Sakamoto et al. 2023*
NEMO4.2-PISCES (IPSL)	*Aumont et al. 2015*
NEMO-PlankTOM12	*Wright et al. 2021*
NorESM1-OCv1.2	*Schwinger et al. 2016*

We convert the reported pCO_2 to fCO_2 [Dickson et al., 2007]. Uncertainty on the LDEO dataset is estimated at $\pm 2.5\mu$atm [Fay et al., 2024].

In the main text, the SOCAT fCO_2 database [Bakker et al., 2016] is used only to remove any points that are also found in the LDEO database. This ensures that no data used to train the observation-based products is included in the independent dataset. In the Supplementary, the GOBMs are compared to an alternative merged dataset that includes SOCAT.

2.2.1 Combination of datasets The independent surface fCO_2 dataset to which we compare the products and GOBMs is a combined set from GLODAP and the LDEO database, after SOCAT points are removed. This dataset is at 1^ox1^o spatial and monthly temporal resolution for 2000-2023. We report the number of points for each of the 5 superbiomes [Fay & McKinley, 2014, Fay & McKinley, 2021] that are the focus for our analysis (Table 2). Due to the extreme sparsity of the independent data, far-northern and southern ice biomes are not considered in this analysis. For the purpose of discussing the datasets in this section, "global" is the union of the 14 non-ice open-ocean biomes, which leaves out coastal zones and marginal seas [Fay & McKinley, 2014]. The timeframe is 2000-2023.

To construct the final dataset, we applied the following data screening and merging steps. First, we remove any outlier points defined as those with fCO_2 higher than 650μatm or lower than 100μatm. This removes 0.7% from GLODAP, 0.02% from SOCAT, 0.02% from LDEO. Second, all points that are found in both the LDEO and SOCAT database are identified. These points are removed. This makes the "LDEOnoSOCAT" dataset (N=11,573, global). Third, to combine with surface ocean GLODAP data (N=1,043, global), we identify any 1^ox1^o monthly points in both GLODAP and "LDEOnoSOCAT". These points are averaged. The remaining 1^ox1^o monthly points in the final dataset are taken from either GLODAP or "LDEO no SOCAT". This creates the "GLODAP+LDEOnoSOCAT" surface ocean dataset that is our primary basis for comparison (N=12,590, global). The final point counts per superbiome are provided in Table 2.

Uncertainty for the combined GLODAP+LDEOnoSOCAT dataset is estimated at 4.2μatm using the square root of the weighted sum of squares, with the weighting being the percentage of data from GLODAP (8%) and LDEOnoSOCAT (92%).

Table 2. Superbiomes and the number of independent datapoints in GLODAP+LDEOnoSOCAT for 2000-2023. Superbiomes are visualized in the inset maps in Figures 4 and 5. The original biomes of [Fay & McKinley, 2014] that are merged to create each superbiome are also indicated.

Superbiome	**Biomes**	**Datapoints**
North Seasonally Stratified (N.SS)	2,3,9,10	3,892
North Subtropical Permanently Stratified (N.STPS)	4,11	3,557
Equatorial (Eq)	5,6,12	1,374
South Subtropical Permanently Stratified (S.STPS)	7,13,14	1,723
Southern Ocean (S.Ocean)	15,16	1,242

In the Supplementary (Section 5), we compare the GOBMs to an alternative dataset where SOCAT points are not removed. This alternative merged dataset is 23 times larger than GLODAP+LDEOnoSOCAT, but cannot be used for our primary comparisons because the observation-based products are trained with the SOCAT data.

2.3 Comparing to independent data

The sparse surface ocean independent data in GLODAP+LDEOnoSOCAT are used at 1^ox1^o spatial and monthly temporal resolution. These points are extracted individually from each observation-based product and GOBM. We apply the removal of outliers procedure as applied to the independent data (Section 2.2.1) in which we remove any outlier points from the products and GOBMs with fCO_2 lower than 100 μatm or higher than 650 μatm.

Both independent data and the points extracted from the products or GOBMs are aggregated over 'superbiomes' (Table 2) using an area-weighted average. This leads to a timeseries for each superbiome for the independent data, for each product and for each GOBM. In each case, the trend of atmospheric xCO_2 from NOAA ERSL global marine boundary layer product is used to detrend the timeseries [Lan et al., 2024]. A monthly climatology from the detrended timeseries is constructed by averaging all data in each month ('seasonal'). The detrended non-seasonal variability ('variability') is calculated by removing both the trend and the annually-repeating climatology. Figure 3 provides a visual representation of this analysis.

2.4 Statistical measures of skill

Bias is calculated as the mean of the Prediction minus the mean of the Observation (bias = $\overline{P} - \overline{O}$). The sign of the bias indicates whether the Prediction (product or GOBM) overestimates (positive) or underestimates (negative) fCO_2.

Unbiased root mean squared error (uRMSE) measures the magnitude of the predicted error after the bias is removed. uRMSE penalizes larger errors and outliers. It is calculated as the square root of the mean of the squared unbiased error (uRMSE=$\sqrt{\overline{[(P - bias) - O]^2}}$).

The Pearson correlation coefficient (r) measures how much the product or GOBM varies consistently with the independent data. Values near +1 indicate high tendency to vary together. It is calculated as the covariance between the predictions and the observations, divided by the product of their individual standard deviations.

All statistical analyses are done for each individual member of the 10 member ensembles for each products and GOBMs (Tables 1, 2). The presentation focuses on the mean and spread (1σ) of each metric for the suite of products or GOBMs in each superbiome.

3 Results

The large spread in surface fCO_2 estimates across observation-based products and GOBMs for a single month is demonstrated by the 1σ spread of the 10 ensemble members for January and July of 2015 (Figure 1). For both months, the observation-based products are more consistent in their estimates across most of the ocean, with 1σ values as low as a few μatm in the central subtropical gyres of the Northern Hemisphere and <10 μatm in the central subtropical gyres of the Southern Hemisphere. In the far eastern equatorial Pacific, in the Arctic, and along the coasts, the 1σ spread exceeds 20μatm in the products. The winter hemisphere tends to have a reduced spread compared to the summer hemisphere. The spread across the GOBMs is greater everywhere, exceeding 10μatm in the central subtropical gyres of both hemispheres and exceeding 25μatm over large swaths of the ocean, particularly in high latitude summer. The Arctic and coastal regions of GOBMs generally have the largest 1σ spread, exceeding 25μatm. In summary, we find a lack of agreement among ensemble members at monthly temporal and 1^ox1^o spatial resolution for both observation-based products and GOBMs, with the degree of disagreement across the ensemble being greater for GOBMs.

Our goal here is to assess the skill of the observation-based products and GOBMs using co-located independent data. In Figure 2, the sparsity of these data is illustrated with the 2000-2023 mean of one product differenced from the GLODAP+LDEOnoSOCAT independent data (Figure 2a) and of one GOBM differenced from the same (Figure 2b). Independent data are more numerous in the Northern Hemisphere and tropical Pacific. The Indian Ocean and the Southern Hemisphere are particularly sparse.

Our treatment of the data, described in Section 2.3, is illustrated using the Northern Seasonally Stratified (N.SS) superbiome in Figure 3. The individual observation-based products and GOBMs are sampled for the same month and 1^ox1^o locations where independent data exist (Figure 2). For

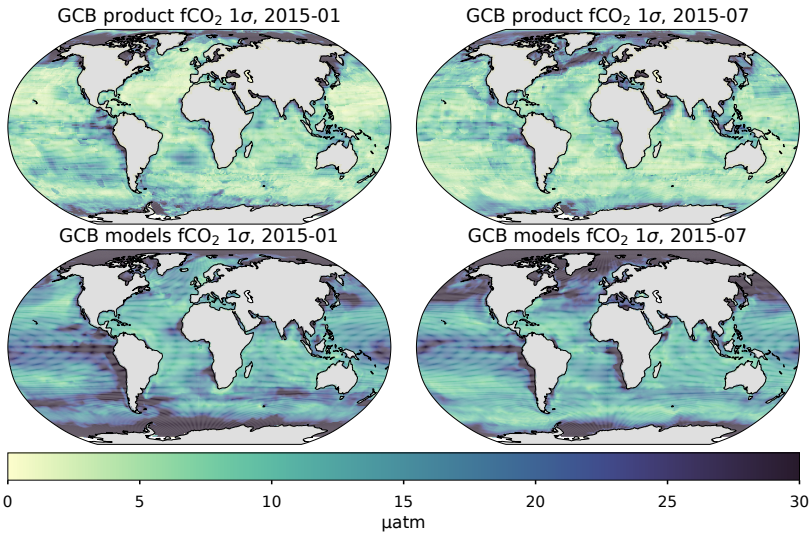

Figure 1. Spread of products and Models in January and July 2015

each superbiome, these data are collapsed to a single timeseries (Figure 3a,d). A linear trend is calculated from the full timeseries (Table 3). A seasonal climatology is created from the superbiome timeseries (Figure 3b,e). The detrended non-seasonal variability (Figure 3c,f) is the remainder after the linear trend and annually-repeating climatology are removed.

Table 3. fCO_2 trends for 2000-2023 (μatm/yr) for each superbiome region and for the independent dataset GLODAP+LDEOnoSOCAT. For the observation-based products and the GOBMs, the ensemble mean $\pm$ the ensemble standard deviation are reported.

Superbiome	**GLODAP+LDEOnoSOCAT**	**Products**	**GOBMs**
N.SS	2.2	2.1 $\pm$ 0.03	2.1 $\pm$ 0.03
N.STPS	2.0	2.1 $\pm$ 0.01	2.1 $\pm$ 0.01
Eq	2.0	2.0 $\pm$ 0.04	2.0 $\pm$ 0.05
S.STPS	2.1	2.1 $\pm$ 0.01	2.1 $\pm$ 0.02
S.Ocean	2.0	2.0 $\pm$ 0.05	2.1 $\pm$ 0.03

In the N.SS, independent data exist for most months prior to 2015 and then become more sparse (Figure 3a,d). Visual comparison of the seasonality (Figure 3b,e) indicates that products capture the independent observations with far greater fidelity than the GOBMs. It is not possible to visually assess skill with respect to the variability from Figure 3(c,f).

Trends for the independent data and for the products and the GOBMs are nearly identical, ranging from 2.0-2.2 μatm/yr across the superbiomes (Table 3). The strongly forced response of ocean fCO_2 to rapidly rising atmospheric CO_2 concentrations [McKinley et al., 2020, DeVries et al., 2023] is a consistent signal across the independent datasets, observation-based products, and GOBMs for all superbiomes.

For quantitative comparisons of skill against GLODAP+LDEOnoSOCAT, we turn to Figures 4 and 5. Greater skill is indicated by lower bias, lower RMSE and a higher correlation coefficient (r). For observation-based products, the ensemble mean bias ranges from -3 to +6μatm, while for the GOBMs, ensemble mean bias ranges from +1 to +13μatm (Figure 4). The full spread of GOBM bias is large compared to the products. This is a main difference between the products and the GOBMs. Bias in individual products ranges from value of -4 to +9μatm, while GOBM bias spans a

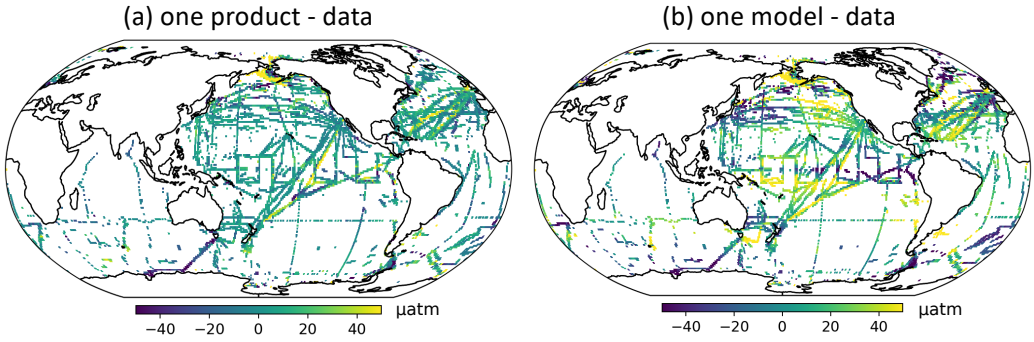

Figure 2. Example surface fCO_2 difference (in μatm) of (a) one product (SOM-FFN) and (b) one model (FESOM-RECOM) from the GLODAP+LDEOnoSOCAT independent data, mean for 2000-2023. Positive (negative) values indicate high (low) bias relative to observations.

much larger range, from -18 to +32μatm. In contrast to the GOBMs, the products have bias tightly clustered within a few μatm of the ensemble mean.

The highest uRMSE occurs in the N.SS superbiome (Figure 5a). For the full timeseries ('All'), the bias for products ranges from 30-45μatm, with an ensemble mean of 37μatm. For the GOBMs, the range is 50-60μatm with an ensemble mean of 57μatm for GOBMs). The smallest uRMSEs are found in the two subtropical superbiomes (Figure 5b,d). For each ensemble member, the uRMSE for the products is always closer to the ensemble mean than for the GOBMs. Ensemble-mean correlations for the products are also always higher than for the GOBMs. Notably, in the high-latitude superbiomes (N.SS and SO), the ensemble-mean correlation for the products exceeds 0.6, while the ensemble-mean correlation for the GOBMs is always 0.3 or less.

In the subtropics, ensemble-mean correlations for the full timeseries are reasonably high for both GOBMs and products: >0.75 for the Southern Subtropical Permanently Stratified (S.STPS, Figure 5d), and >0.65 in the Northern Subtropical Permanently Stratified (N.STPS, Figure 5b). In these superbiomes, the ensemble-mean uRMSE is ~20μatm for the products and ~25μatm for the GOBMs.

In the equatorial superbiome, when considering the full timeseries, the products all perform better than even the best performing GOBMs in terms of both uRMSE and correlation (Figure 5c). The products have a mean uRMSE of 23μatm and mean correlation of 0.85, while the GOBMs have a mean uRMSE of 35μatm and mean correlation of 0.65.

In all superbiomes, most of the uRMSE and most of the correlation comes from the biome-aggregated seasonal cycle. This is shown with the central pair of bars ('Seasonal') in each sub-panel of Figure 5 being only modestly smaller than the left pair ('All'). This finding is consistent with seasonality being the main signal of variation in surface ocean fCO_2 [Takahashi et al., 1993], a signal captured by both the products and the GOBMs (Figure 3), though with substantial residual errors against these independent data (Figure 5).

The detrended non-seasonal variability has smaller mean uRMSEs (<13μatm) and low ensemble-mean correlations <0.3 in all superbiomes (Figure 5). Ensemble-mean correlations for the

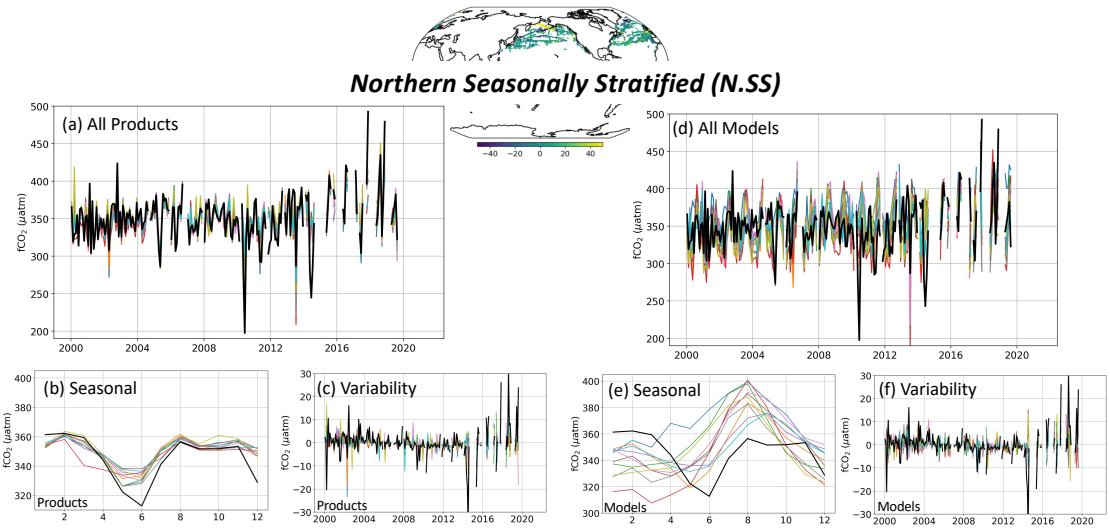

Figure 3. Visualization of the analysis, for the Northern Seasonally Stratified (N.SS) superbiome. See text for further description.

products are higher than for the GOBMs, with the exception of N.STPS, where they are indistinguishable. In N.STPS and N.SS, the spread of the individual product correlations is larger than the spread of the GOBMs, while in Eq, the opposite is true. In S.STPS and SO, the spread across products and across GOBMs are comparable.

These comparisons use GLODAP+LDEOnoSOCAT as independent data, allowing the relative skill of the products and GOBMs to be directly compared. However, the SOCAT database offers a much larger dataset from which the GOBMs are independent. In the Supplementary, comparisons for the GOBMs are repeated with the inclusion of the SOCAT data [Bakker et al., 2016]. Qualitatively, the comparisons are similar, but there are quantiative differences. Against GLODAP+LDEO+SOCAT, the GOBMs have similar biases and slightly improved performance for the full timeseries and seasonality in terms of uRMSE and r. For the variability, comparison to GLODAP+LDEO+SOCAT suggests modestly higher uRMSE and correlations in all superbiomes. For more discussion, please see the Supplementary Material.

4 Discussion and Conclusion

These comparisons to independent fCO_2 data demonstrate that the GOBM ensemble is less skillfull than the product ensemble in all superbiomes. For both products and GOBMs, biases are often larger than the estimated uncertainty of the independent dataset ($\pm 4\mu$atm), and uRMSEs are always larger for the full timeseries ('All') and the dominant timescale ('Seasonal'). Another important finding is that individual products tend to group together around the product ensemble mean much more tightly than the individual GOBMs around their ensemble mean. In other words, the products are more consistent in their skill than the GOBMs.

In all 5 superbiomes and for both products and GOBMs, deviations from independent observations, quantified with uRMSE, are at least 1 order of magnitude larger than maximum expected signals in recent mCDR modeling studies focused on hypothetical ocean alkalinity enhancement (OAE) deployments [Wang et al., 2022, Zhou et al., 2024]. Significant improvements will be required before these products and GOBMs could be used to assess the counterfactual for the ocean carbon sink and for mCDR additionality to be determined with these estimates as a

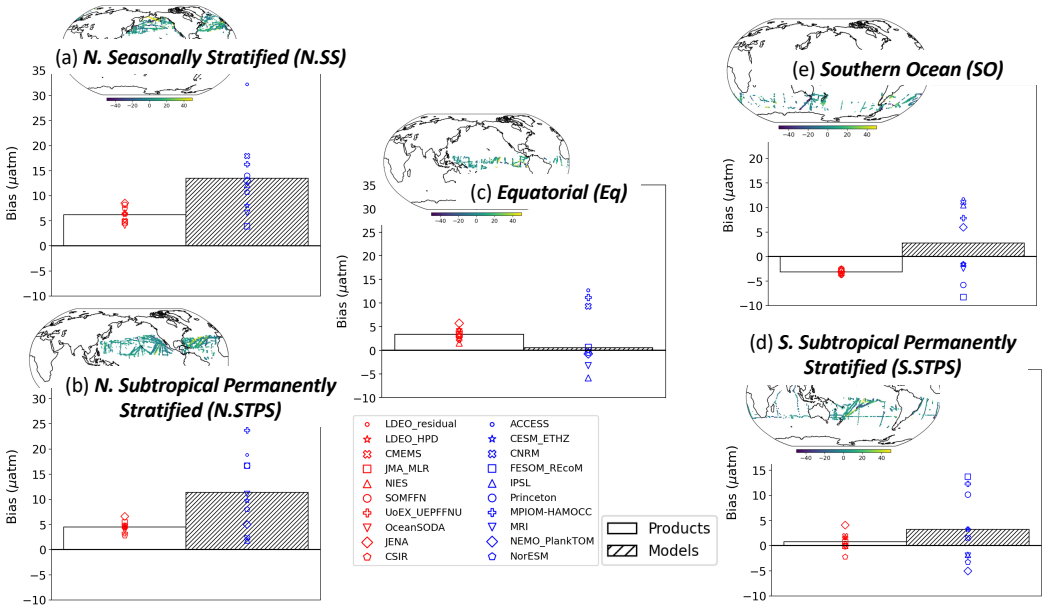

Figure 4. Bias against GLODAP+LDEOnoSOCAT independent data. Products are the open bars with red symbols, models are the hatched bars with blue symbols. NorESM has an extreme negative bias (-17.7μatm) in the Equatorial biome that is not shown to improve the figure's overall appearance.

reference state.

Across the superbiomes, we find substantial biases in 2000-2023 long-term mean fCO_2. Biases are substantially larger in GOBMs than in the products (Figure 4), and with a much larger ensemble spread. This is consistent with much larger spread in the mean ocean carbon sink estimated by the GOBMs compared to the products [Terhaar et al., 2024]. Both superbiomes of the Northern Hemisphere have positive ensemble mean GOBM fCO_2 biases greater than +10μatm against GLODAP+LDEOnoSOCAT (Figure 4) and smaller, but still positive against the merged independent dataset that includes SOCAT data (Figure S3). Most GOBMs do not include fluxes of natural carbon from the land to the ocean via rivers [Regnier et al., 2022] that should raise fCO_2 and lead to CO_2 outgassing. Since this process is weak or missing in these GOBMs [DeVries et al., 2023], GOBM underestimation of surface ocean fCO_2 could be expected. Instead, we find predominantly overestimation of fCO_2 (Figures 4 and S2).

The recent RECCAP2 assessment also found significant discrepancies in the GOBMs compared to the products [Terhaar et al., 2024, DeVries et al., 2023]. Terharr et al. (2024) attribute GOBM biases to model spinup, ocean circulation, and chemistry errors. Many members of the CMIP5 Earth System Models (ESM) suite underestimate carbon uptake in the North Atlantic, with seasonal mechanisms being critical [Goris et al., 2018]. CMIP6 ESMs have substantial mean state discrepancies for the historical period compared to a similar suite of products. These errors are largely preserved in future projections and are responsible for at least 50% of the projection uncertainty with respect to the ocean carbon sink [McKinley et al., 2023]. This study adds to this accumulating evidence that GOBMs, and their closely-related ESM cousins, overestimate surface ocean fCO_2 and thus underestimate the mean ocean carbon sink. Given the mounting evidence of substantial GOBM errors, a recent publication [Friedlingstein et al., 2026] proposes that the Global Carbon Budget adjust the ocean carbon sink estimated by GOBMs: essentially increasing them by 10%. This adjustment is used in the most recent Global Carbon Budget release [Friedlingstein et al., 2025a, McKinley, 2026].

There are a handful of ocean biogeochemical models that use data assimilation in an attempt to

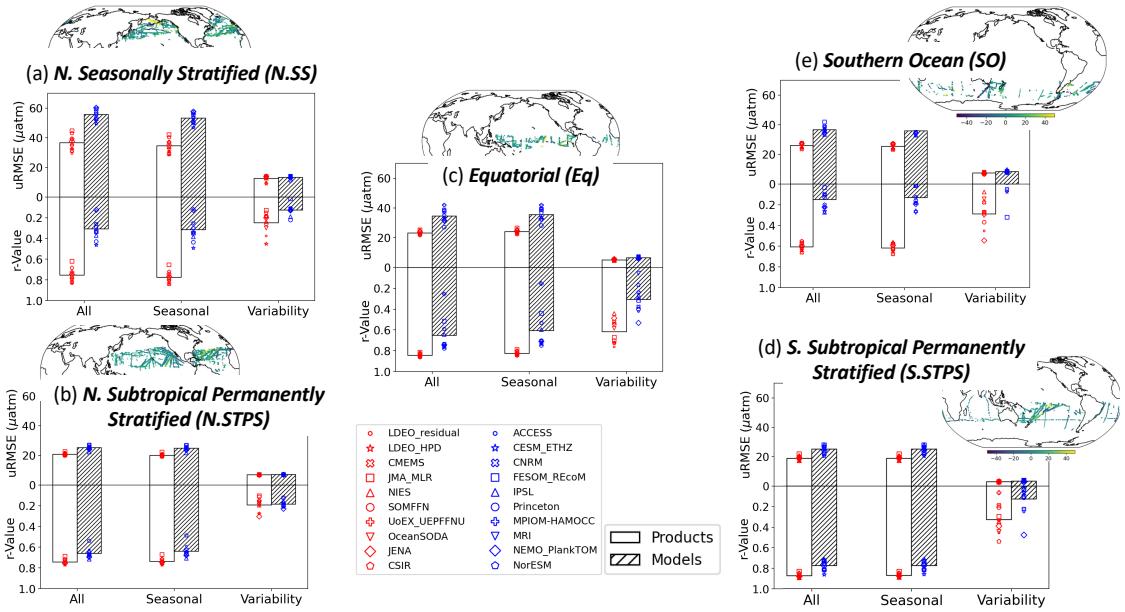

Figure 5. Unbiased Root-Mean-Square Error (uRMSE) and Correlation (r) against GLODAP+LDEOnoSOCAT independent data. In each subpanel, the first set of bars is for the full dataset (All), the second for the seasonality, and the third for the remaining non-seasonal variability (Section 2.3 and Figure 1). The top half of each panel shows uRMSE and the bottom shows correlation. Products are the open bars with red symbols, models are the hatched bars with blue symbols. If the ensemble-mean correlation is negative, no bar is shown.

increase fidelity. In the ECCO family of models, the adjoint method is used to adjust the physical model state and then a Green's Function approach is used with data such as GLODAP and SOCAT to adjust parameters of the biogeochemical module [Carroll et al., 2020, Carroll et al., 2022, Moseley et al., 2026]. Could such data assimilation efforts substantially improve these comparisons shown here? In Section S.4, we extend these comparisons to two models in the ECCO family and do not find significant improvements.

Observation-based products are generally more skillful than GOBMs, but also have substantial uncertainties that need to be addressed with additional data collection and algorithmic improvements [Heimdal et al., 2026]. For example, uRMSEs are 37μatm in the Northern Seasonaly Stratitifed superbiome (N.SS), and at least 20μatm in other superbiomes. Non-seasonal variability is smaller magnitude and poorly represented. (Figure 5).

Despite mean state and seasonal discrepancies, both products and GOBMs consistently estimate the trend in fCO_2 in all superbiomes. This is consistent with the very strong forced signal from rising atmospheric CO_2 concentrations [McKinley et al., 2020, Gruber et al., 2023, DeVries et al., 2023].

Seasonality is where there is some skill in terms of phasing (modest to high correlations), but at the same time where there remains substantial lack of fidelity in both products and GOBMs (uRMSE) (Figure 5). This is particularly true for the GOBMs and, at higher latitudes, for both products and GOBMs (Figures 3, 5). It is important to acknowledge that aggregation of the sparse data to a superbiome timeseries before estimation of the seasonal cycle means that not all of the 'seasonal' variation is strictly temporal. Instead, some of the variation is due to the spatial heterogeneity of sampling. Comparison of the biome-aggregated timeseries of Northern Subtropical Permanently Stratified (N.STPS) biome to the timeseries at BATS and HOT suggests that spatial impacts may play a significant role (Section S.5). Prior studies that have attributed seasonal errors in GOBM fCO_2 to errors in the representation of physical and biological processes associated with

dissolved inorganic carbon (DIC) cycling, that are spatially heterogeneous across the gyres [Mongwe et al., 2018, Rodgers et al., 2023, DeVries et al., 2023]. Since the products offer more reliable estimates of seasonal amplitude, phase and the spatial distribution of fCO_2 [Gloege et al., 2021], they should be very useful to guide the next steps of GOBM development.

Errors in non-seasonal variability are relatively small in terms of uRMSEs. The phasing of this variability is poorly estimated by both products and GOBMs, with the exception of the products in the equatorial superbiome where the ensemble mean correlation is 0.6 (Figure 5). Given the sparsity of the independent data (Table 2), we do not attempt to determine the extent to which non-seasonal variability is due to long-term variability as opposed to high-frequency events such as storms, fronts and eddies. Sustained observations that can better constrain non-seasonal variability will be needed to make future progress in this area.

In this study, we compare observation-based products and GOBMs to the same independent dataset. Though these data are sparse, they are global in scope and fully independent of the products. The products are more skillful than the GOBMs, with lower bias, lower uRMSEs and higher correlation to the independent data. Biome-aggregated seasonal signals are dominant and non-seasonal variability is smaller and poorly represented. A key future direction is to improve the representation of fCO_2 seasonality in GOBMs and to collect more surface ocean fCO_2 data to both improve observation-based products and to expand independent datasets for more comprehensive skill assessments.

5 Data Availability

The observation-based products and GOBMs from the Global Carbon Budget 2024 are available at https://zenodo.org/records/14092497. The LDEO-Residual product is available at https://oceancarbon.ldeo.columbia.edu. GLODAP is available from https://glodap.info/index.php/merged-and-adjusted-data-product-v2-2023/. LDEO pCO_2 database is available via NCEI at https://www.ncei.noaa.gov/access/ocean-carbon-acidification-data-system/oceans/LDEO_Underway_Database/. SOCATv2024 database is available at https://socat.info/index.php/version-2024/.

Acknowledgments

GAM conceived of the study, conducted the analysis and drafted the manuscript. Other authors contributed datasets, code and revised the manuscript. We acknowledge support from the National Oceanic and Atmospheric Administration (NA24OARX431G0151-T1-01); the National Aeronautic and Space Administration (80NSSC22K0150); and the National Science Foundation through the LEAP Science Technology Center (AGS-2019625) and from award OCE-2333608. We acknowledge support from Schmidt Sciences, LLC, and thank the COCO2 team for their collective efforts in data collection and machine learning development. The Surface Ocean CO_2 Atlas (SOCAT) is an international effort, endorsed by the SCOR Infrastructural Project International Ocean Carbon Coordination Project (IOCCP) and the Surface Ocean Lower-Atmosphere Study (SOLAS), to deliver a uniform, quality-controlled surface ocean CO_2 database. The many researchers and funding agencies responsible for the collection of data and quality control are thanked for their contributions to SOCAT.

References

[Aumont et al., 2015] Aumont, O., Ethé, C., Tagliabue, A., Bopp, L., & Gehlen, M. (2015). Pisces-v2: an ocean biogeochemical model for carbon and ecosystem studies. *Geoscientific Model Development*, 8, 2465–2513.

[Bakker et al., 2016] Bakker, D. C. E., Pfeil, B., Landa, C. S., Metzl, N., O'Brien, K. M., Olsen, A., Smith, K., Cosca, C., Harasawa, S., Jones, S. D., Nakaoka, S., Nojiri, Y., Schuster, U., Steinhoff, T., Sweeney, C., Takahashi, T., Tilbrook, B., Wada, C., Wanninkhof, R., Alin, S. R., Balestrini, C. F., Barbero, L., Bates, N. R., Bianchi, A. A., Bonou, F., Boutin, J., Bozec, Y., Burger, E. F., Cai, W.-J., Castle, R. D., Chen, L., Chierici, M., Currie, K., Evans, W., Featherstone, C., Feely, R. A., Fransson, A., Goyet, C., Greenwood, N., Gregor, L., Hankin, S., Hardman-Mountford, N. J., Harlay, J., Hauck, J., Hoppema, M., Humphreys, M. P., Hunt, C. W., Huss, B., Ibánhez, J. S. P., Johannessen, T., Keeling, R., Kitidis, V., Körtzinger, A., Kozyr, A., Krasakopoulou, E., Kuwata, A., Landschützer, P., Lauvset, S. K., Lefèvre, N., Lo Monaco, C., Manke, A., Mathis, J. T., Merlivat, L., Millero, F. J., Monteiro, P. M. S., Munro, D. R., Murata, A., Newberger, T., Omar, A. M., Ono, T., Paterson, K., Pearce, D., Pierrot, D., Robbins, L. L., Saito, S., Salisbury, J., Schlitzer, R., Schneider, B., Schweitzer, R., Sieger, R.,

Skjelvan, I., Sullivan, K. F., Sutherland, S. C., Sutton, A. J., Tadokoro, K., Telszewski, M., Tuma, M., van Heuven, S. M. A. C., Vandemark, D., Ward, B., Watson, A. J., & Xu, S. (2016). A multi-decade record of high-quality fCO_2 data in version 3 of the Surface Ocean CO_2 Atlas (SOCAT). *Earth System Science Data*, 8(2), 383–413.

[Bates et al., 2014a] Bates, N. R., Astor, Y. M., Church, M. J., Currie, K., Dore, J. E., González-Dávila, M., et al. (2014a). A time-series view of changing ocean chemistry due to ocean uptake of anthropogenic CO2 and ocean acidification. *Oceanography*, 27(1), 126–141.

[Bates et al., 2014b] Bates, N. R., Johnson, R. J., Accornero, A., Bidigare, R. R., Close, A. R., Hansell, D. A., Jenkins, W. J., Michaels, A. F., O'Brien, T. D., Parsons, R. J., & Steinberg, D. K. (2014b). Bermuda atlantic time-series study (bats): Research and results from 1988–2012. *Deep-Sea Research Part II: Topical Studies in Oceanography*, 93, 1–8.

[Bennington et al., 2022a] Bennington, V., Galjanic, T., & McKinley, G. A. (2022a). Explicit physical knowledge in machine learning for ocean carbon flux reconstruction: The pCO2-Residual method. *Journal of Advances in Modeling Earth Systems*, e2021MS002960.

[Bennington et al., 2022b] Bennington, V., Gloege, L., & McKinley, G. A. (2022b). Variability in the global ocean carbon sink from 1959 to 2020 by correcting models with observations. *Geophysical Research Letters*, 49(14), e2022GL098632. e2022GL098632 2022GL098632.

[Berthet et al., 2019] Berthet, S., Séférian, R., Bricaud, C., Chevallier, M., Voldoire, A., & Ethé, C. (2019). Evaluation of an online grid-coarsening algorithm in a global eddy-admitting ocean biogeochemical model. *Journal of Advances in Modeling Earth Systems*, 11(6), 1759–1783.

[Canadell et al., 2021] Canadell, J., Monteiro, P., Costa, M., Cunha, L. C. d., Cox, P., Eliseev, A., Henson, S., Ishii, M., Jaccard, S., Koven, C., Lohila, A., Patra, P., Piao, S., Rogelj, J., Syampungani, S., Zaehle, S., & Zickfeld, K. (2021). *IPCC AR6, Chapter 6, Global Carbon and other Biogeochemical Cycles and Feedbacks*. Technical report, Cambridge University Press.

[Carroll et al., 2020] Carroll, D., Menemenlis, D., Adkins, J. F., Bowman, K. W., Brix, H., Dutkiewicz, S., & et al. (2020). The ECCO-Darwin data-assimilative global ocean biogeochemistry model: Estimates of seasonal to multi-decadal surface ocean pCO_2 and air-sea CO_2 flux. *Journal of Advances in Modeling Earth Systems*, 12(10), e2019MS001888.

[Carroll et al., 2022] Carroll, D., Menemenlis, D., Dutkiewicz, S., Lauderdale, J. M., Adkins, J. F., Bowman, K. W., Brix, H., Fenty, I., Gierach, M. M., Hill, C., Jahn, O., Landschützer, P., Manizza, M., Mazloff, M. R., Miller, C. E., Schimel, D. S., Verdy, A., Whitt, D. B., & Zhang, H. (2022). Attribution of space-time variability in global-ocean dissolved inorganic carbon. *Global Biogeochemical Cycles*, 36(3), e2021GB007162. e2021GB007162 2021GB007162.

[Chau et al., 2022] Chau, T. T. T., Gehlen, M., & Chevallier, F. (2022). A seamless ensemble-based reconstruction of surface ocean pCO2 and air–sea CO2 fluxes over the global coastal and open oceans. *Biogeosciences*, 19(4), 1087–1109.

[DeVries et al., 2023] DeVries, T., Yamamoto, K., Wanninkhof, R., Gruber, N., Hauck, J., Müller, J. D., Bopp, L., Carroll, D., Carter, B., Chau, T., Doney, S. C., Gehlen, M., Gloege, L., Gregor, L., Henson, S., Kim, J. H., Iida, Y., Ilyina, T., Landschützer, P., Quéré, C. L., Munro, D., Nissen, C., Patara, L., Pérez, F. F., Resplandy, L., Rodgers, K. B., Schwinger, J., Séférian, R., Sicardi, V., Terhaar, J., Triñanes, J., Tsujino, H., Watson, A., Yasunaka, S., & Zeng, J. (2023). Magnitude, Trends, and Variability of the Global Ocean Carbon Sink From 1985 to 2018. *Global Biogeochemical Cycles*, 37(10).

[Dickson et al., 2007] Dickson, A. G., Sabine, C. L., & Christian, J. R. (2007). *Guide to best practices for ocean CO_2 measurements*. North Pacific Marine Science Organization.

[Doney et al., 2009] Doney, S. C., Lima, I., Feely, R. A., Glover, D. M., Lindsay, K., Mahowald, N., Moore, J. K., & Wanninkhof, R. (2009). Mechanisms governing interannual variability in upper-ocean inorganic carbon system and air-sea CO_2 fluxes: Physical climate and atmospheric dust. *Deep Sea Research Part II: Topical Studies in Oceanography*, 56(8), 640–655. Surface Ocean CO2 Variability and Vulnerabilities.

[Fay & McKinley, 2014] Fay, A. R. & McKinley, G. A. (2014). Global open-ocean biomes: mean and temporal variability. *Earth System Science Data*, 6, 273–284.

[Fay & McKinley, 2021] Fay, A. R. & McKinley, G. A. (2021). Observed Regional Fluxes to Constrain Modeled Estimates of the Ocean Carbon Sink. *Geophysical Research Letters*, 48(20).

[Fay et al., 2024] Fay, A. R., Munro, D. R., McKinley, G. A., Pierrot, D., Sutherland, S. C., Sweeney, C., & Wanninkhof, R. (2024). Updated climatological mean fCO2 and net sea–air CO2 flux over the global open ocean regions. *Earth System Science Data*.

[Ford et al., 2024] Ford, D. J., Blannin, J., Watts, J., Watson, A. J., Landschützer, P., Jersild, A., & Shutler, J. D. (2024). A Comprehensive Analysis of Air-Sea CO2 Flux Uncertainties Constructed From Surface Ocean Data Products. *Global Biogeochemical Cycles*.

[Friedlingstein et al., 2025a] Friedlingstein, P., O'Sullivan, M., Jones, M. W., Andrew, R. M., Bakker, D. C. E., Hauck, J., Landschützer, P., Quéré, C. L., Li, H., Luijkx, I. T., Peters, G. P., Peters, W., Pongratz, J., Schwingshackl, C., Sitch, S., Canadell, J. G., Ciais, P., Aas, K., Alin, S. R., Anthoni, P., Barbero, L., Bates, N. R., Bellouin, N., Benoit-Cattin, A., Berghoff, C. F., Bernardello, R., Bopp, L., Brasika, I. B. M., Chamberlain, M. A., Chandra, N., Chevallier, F., Chini, L. P., Collier, N. O., Colligan, T. H., Cronin, M., Djeutchouang, L., Dou, X., Enright, M. P., Enyo, K., Erb, M., Evans, W., Feely, R. A., Feng, L., Ford, D. J., Foster, A., Fransner, F., Gasser, T., Gehlen, M., Gkritzalis, T., Souza, J. G. D., Grassi, G., Gregor, L., Gruber, N., Guenet, B., Gürses, , Harrington, K., Harris, I., Heinke, J., Hurtt, G. C., Iida, Y., Ilyina, T., Ito, A., Jacobson, A. R., Jain, A. K., Jarníková, T., Jersild, A., Jiang, F., Jones, S. D., Kato, E., Keeling, R. F., Goldewijk, K. K., Knauer, J., Kong, Y., Korsbakken, J. I., Koven, C., Kunimitsu, T., Lan, X., Liu, J., Liu, Z., Liu, Z., Monaco, C. L., Ma, L., Marland, G., McGuire, P. C., McKinley, G. A., Melton, J., Monacci, N., Monier, E., Morgan, E. J., Munro, D. R., Müller, J. D., Nakaoka, S.-I., Nayagam, L. R., Niwa, Y., Nutzel, T., Olsen, A., Omar, A. M., Pan, N., Pandey, S., Pierrot, D., Qin, Z., Regnier, P. A. G., Rehder, G., Resplandy, L., Roobaert, A., Rosan, T. M., Rödenbeck, C., Schwinger, J., Skjelvan, I., Smallman, T. L., Spada, V., Sreeush, M. G., Sun, Q., Sutton, A. J., Sweeney, C., Swingedouw, D., Séférian, R., Takao, S., Tatebe, H., Tian, H., Tian, X., Tilbrook, B., Tsujino, H., Tubiello, F., Ooijen, E. v., Werf, G. v. d., Velde, S. J. v. d., Walker, A., Wanninkhof, R., Yang, X., Yuan, W., Yue, X., & Zeng, J. (2025a). Global Carbon Budget 2025. *Earth System Science Data Discussions*, 2025, 1–139.

[Friedlingstein et al., 2025b] Friedlingstein, P., O'Sullivan, M., Jones, M. W., Andrew, R. M., Hauck, J., Landschützer, P., Quéré, C. L., Li, H., Luijkx, I. T., Olsen, A., Peters, G. P., Peters, W., Pongratz, J., Schwingshackl, C., Sitch, S., Canadell, J. G., Ciais, P., Jackson, R. B., Alin, S. R., Arneth, A., Arora, V., Bates, N. R., Becker, M., Bellouin, N., Berghoff, C. F., Bittig, H. C., Bopp, L., Cadule, P., Campbell, K., Chamberlain, M. A., Chandra, N., Chevallier, F., Chini, L. P., Colligan, T., Decayeux, J., Djeutchouang, L. M., Dou, X., Rojas, C. D., Enyo, K., Evans, W., Fay, A. R., Feely, R. A., Ford, D. J., Foster, A., Gasser, T., Gehlen, M., Gkritzalis, T., Grassi, G., Gregor, L., Gruber, N., Gürses, , Harris, I., Hefner, M., Heinke, J., Hurtt, G. C., Iida, Y., Ilyina, T., Jacobson, A. R., Jain, A. K., Jarníková, T., Jersild, A., Jiang, F., Jin, Z., Kato, E., Keeling, R. F., Goldewijk, K. K., Knauer, J., Korsbakken, J. I., Lan, X., Lauvset, S. K., Lefèvre, N., Liu, Z., Liu, J., Ma, L., Maksyutov, S., Marland, G., Mayot, N., McGuire, P. C., Metzl, N., Monacci, N. M., Morgan, E. J., Nakaoka, S.-I., Neill, C., Niwa, Y., Nützel, T., Olivier, L., Ono, T., Palmer, P. I., Pierrot, D., Qin, Z., Resplandy, L., Roobaert, A., Rosan, T. M., Rödenbeck, C., Schwinger, J., Smallman, T. L., Smith, S. M., Sospedra-Alfonso, R., Steinhoff, T., Sun, Q., Sutton, A. J., Séférian, R., Takao, S., Tatebe, H., Tian, H., Tilbrook, B., Torres, O., Tourigny, E., Tsujino, H., Tubiello, F., Werf, G. v. d., Wanninkhof, R., Wang, X., Yang, D., Yang, X., Yu, Z., Yuan, W., Yue, X., Zaehle, S., Zeng, N., & Zeng, J. (2025b). Global Carbon Budget 2024. *Earth System Science Data*, 17(3), 965–1039.

[Friedlingstein et al., 2026] Friedlingstein, P., Quéré, C. L., O'Sullivan, M., Hauck, J., Landschützer, P., Luijkx, I. T., Li, H., Woude, A. v. d., Schwingshackl, C., Pongratz, J., Regnier, P., Andrew, R. M., Bakker, D. C. E., Canadell, J. G., Ciais, P., Gasser, T., Jones, M. W., Lan, X., Morgan, E., Olsen, A., Peters, G. P., Peters, W., Sitch, S., & Tian, H. (2026). Emerging climate impact on carbon sinks in a consolidated carbon budget. *Nature*, 649(8095), 98–103.

[Gloege et al., 2021] Gloege, L., McKinley, G. A., Landschützer, P., Fay, A. R., Frölicher, T. L., Fyfe, J. C., Ilyina, T., Jones, S., Lovenduski, N. S., Rodgers, K. B., Schlunegger, S., & Takano, Y. (2021). Quantifying Errors in Observationally Based Estimates of Ocean Carbon Sink Variability. *Global Biogeochemical Cycles*, 35(4), e2020GB006788.

[Gloege et al., 2022] Gloege, L., Yan, M., Zheng, T., & McKinley, G. A. (2022). Improved Quantification of Ocean Carbon Uptake by Using Machine Learning to Merge Global Models and pCO_2 Data. *Journal of Advances in Modeling Earth Systems*, 14(2), e2021MS002620. e2021MS002620 2021MS002620.

[Goris et al., 2018] Goris, N., Tjiputra, J. F., Olsen, A., Schwinger, J., Lauvset, S. K., & Jeansson, E. (2018). Constraining projection-based estimates of the future North Atlantic carbon uptake. *Journal of Climate*, 31(10), 3959 – 3978.

[Gregor et al., 2019] Gregor, L., Lebehot, A. D., Kok, S., & Monteiro, P. M. S. (2019). A comparative assessment of the uncertainties of global surface ocean CO_2 estimates using a machine-learning ensemble (CSIR-ML6 version 2019a) – have we hit the wall? *Geoscientific Model Development*, 12, 5113–5136.

[Gregor et al., 2024] Gregor, L., Shutler, J., & Gruber, N. (2024). High-Resolution Variability of the Ocean Carbon Sink. *Global Biogeochemical Cycles*, 38(8).

[Gruber et al., 2023] Gruber, N., Bakker, D., DeVries, T., Gregor, L., Hauck, J., Landschützer, P., McKinley, G., & Müller, J. (2023). Trends and variability in the ocean carbon sink. *Nature Reviews Earth and Environment*, 4, 119–134.

[Heimdal et al., 2026] Heimdal, T. H., Fay, A. R., Shaum, A. P., Acquaviva, V., Bennington, V., Sharples, A. E., Joenson, N. M., & McKinley, G. A. (2026). An update of the LDEO fCO_2-residual method: algorithmic choices improve ocean carbon sink. *Machine Learning: Earth*. Preprint under review.

[Iida et al., 2021] Iida, Y., Takatani, Y., Kojima, A., & Ishii, M. (2021). Global trends of ocean CO2 sink and ocean acidification: an observation-based reconstruction of surface ocean inorganic carbon variables. *Journal of Oceanography*, 77(2), 323–358.

[Karl & Church, 2014] Karl, D. M. & Church, M. J. (2014). Microbial oceanography and the hawaii ocean time-series programme. *Nature Reviews Microbiology*, 12(10), 699–713.

[Lacroix et al., 2020] Lacroix, F., Ilyina, T., & Hartmann, J. (2020). Oceanic CO_2 outgassing and biological production hotspots induced by pre-industrial river loads of nutrients and carbon in a global modeling approach. *Biogeosciences*, 17(1), 55–88.

[Lamarque et al., 2026] Lamarque, J.-F., Friedlingstein, P., Osias, B., Strongin, S., Balaji, V., Bowman, K. W., Canadell, J. G., Ciais, P., Cullen, H., Davis, K. J., Doney, S. C., Gurney, K. R., Karspeck, A. R., Koven, C. D., McKinley, G. A., Peters, G. P., Pongratz, J., Stephens, B., & Sweeney, C. (2026). Improved comparability and system-wide verification to support a scalable carbon credit market. *Earth System Dynamics*. Preprint under review.

[Lan et al., 2024] Lan, X., Tans, P., Thoning, K., & NOAA Global Monitoring Laboratory (2024). NOAA Greenhouse Gas Marine Boundary Layer Reference - CO2. Data set. Downloaded August 31, 2025.

[Landschützer et al., 2016] Landschützer, P., Gruber, N., & Bakker, D. C. E. (2016). Decadal variations and trends of the global ocean carbon sink. *Global Biogeochemical Cycles*, 30(10), 1396–1417.

[Landschützer et al., 2020] Landschützer, P., Laruelle, G. G., Roobaert, A., & Regnier, P. (2020). A uniform pco_2 climatology combining open and coastal oceans. *Earth System Science Data*, 12(4), 2537–2553.

[Lauvset et al., 2016] Lauvset, S. K., Key, R. M., Olsen, A., Heuven, S. V., Velo, A., Lin, X., Schirnick, C., Kozyr, A., Tanhua, T., Hoppema, M., Jutterström, S., Steinfeldt, R., Jeansson, E., Ishii, M., Perez, F. F., Suzuki, T., & Watelet, S. (2016). A new global interior ocean mapped climatology: the $1^\circ \times 1^\circ$ GLODAP version 2. *Earth System Science Data*, 8(2), 325 – 340.

[Lauvset et al., 2021] Lauvset, S. K., Lange, N., Tanhua, T., Bittig, H. C., Olsen, A., Kozyr, A., Álvarez, M., Becker, S., Brown, P. J., Carter, B. R., Cunha, L. C. d., Feely, R. A., Heuven, S. v., Hoppema, M., Ishii, M., Jeansson, E., Jutterström, S., Jones, S. D., Karlsen, M. K., Monaco, C. L., Michaelis, P., Murata, A., Pérez, F. F., Pfeil, B., Schirnick, C., Steinfeldt, R., Suzuki, T., Tilbrook, B., Velo, A., Wanninkhof, R., Woosley, R. J., & Key, R. M. (2021). An updated version of the global interior ocean biogeochemical data product, GLODAPv2.2021. *Earth System Science Data*, 13(12), 5565–5589.

[Law et al., 2017] Law, R. M., Ziehn, T., Matear, R. J., Lenton, A., Chamberlain, M. A., Stevens, L. E., Wang, Y.-P., Srbinovsky, J., Bi, D., Yan, H., & Vohralik, P. F. (2017). The carbon cycle in the australian community climate and earth system simulator (access-esm1) – part 1: Model description and pre-industrial simulation. *Geoscientific Model Development*, 10(6), 2567–2590.

[Liao et al., 2020] Liao, E., Resplandy, L., Liu, J., & Bowman, K. W. (2020). Amplification of the Ocean Carbon Sink During El Niños: Role of Poleward Ekman Transport and Influence on Atmospheric CO_2. *Global Biogeochemical Cycles*, 34(9), e2020GB006574.

[McKinley, 2026] McKinley, G. A. (2026). Revised estimates of CO2 sources and sinks improve global carbon accounting. *Nature*.

[McKinley et al., 2023] McKinley, G. A., Bennington, V., Meinshausen, M., & Nicholls, Z. (2023). Modern air-sea flux distributions reduce uncertainty in the future ocean carbon sink. *Environmental Research Letters*.

[McKinley et al., 2020] McKinley, G. A., Fay, A. R., Eddebbar, Y. A., Gloege, L., & Lovenduski, N. S. (2020). External forcing explains recent decadal variability of the ocean carbon sink. *AGU Advances*, 1(2), e2019AV000149. e2019AV000149 2019AV000149.

[McKinley et al., 2016] McKinley, G. A., Pilcher, D. J., Fay, A. R., Lindsay, K., Long, M. C., & Lovenduski, N. S. (2016). Timescales for detection of trends in the ocean carbon sink. *Nature*, 530(7591), 469 – 472.

[Mongwe et al., 2018] Mongwe, N. P., Vichi, M., & Monteiro, P. M. S. (2018). The seasonal cycle of pCO_2 and CO_2 fluxes in the southern ocean: diagnosing anomalies in CMIP5 Earth system models. *Biogeosciences*, 15(9), 2851–2872.

[Moseley et al., 2026] Moseley, L. A., McKinley, G. A., Carroll, D., Menemenlis, D., Dussin, R., & Nguyen, A. T. (2026). The ASTE-BGC data-assimilative regional ocean biogeochemistry model. *Journal of Advances in Modeling Earth Systems*. Preprint under review.

[Müller et al., 2025] Müller, J. D., Gruber, N., Schneuwly, A., Bakker, D. C. E., Gehlen, M., Gregor, L., Hauck, J., Landschützer, P., & McKinley, G. A. (2025). Unexpected decline in the ocean carbon sink under record-high sea surface temperatures in 2023. *Nature Climate Change*, (pp. 1–8).

[NASEM, 2022] NASEM (2022). *A Research Strategy for Ocean-based Carbon Dioxide Removal and Sequestration*. Technical report.

[Olsen et al., 2016] Olsen, A., Key, R. M., Heuven, S. V., Lauvset, S. K., Velo, A., Lin, X., Schirnick, C., Kozyr, A., Tanhua, T., Hoppema, M., Jutterström, S., Steinfeldt, R., Jeansson, E., Ishii, M., Perez, F. F., & Suzuki, T. (2016). The Global Ocean Data Analysis Project version 2 (GLODAPv2) - an internally consistent data product for the world ocean. *Earth System Science Data*.

[Powis et al., 2023] Powis, C. M., Smith, S. M., Minx, J. C., & Gasser, T. (2023). Quantifying global carbon dioxide removal deployment. *Environmental Research Letters*.

[Regnier et al., 2022] Regnier, P., Resplandy, L., Najjar, R. G., & Ciais, P. (2022). The land-to-ocean loops of the global carbon cycle. *Nature*, 603(7901), 401–410.

[Rodgers et al., 2023] Rodgers, K. B., Schwinger, J., Fassbender, A. J., Landschützer, P., Yamaguchi, R., Frenzel, H., Stein, K., Müller, J. D., Goris, N., Sharma, S., Bushinsky, S., Chau, T., Gehlen, M., Gallego, M. A., Gloege, L., Gregor, L., Gruber, N., Hauck, J., Iida, Y., Ishii, M., Keppler, L., Kim, J., Schlunegger, S., Tjiputra, J., Toyama, K., Ayar, P. V., & Velo, A. (2023). Seasonal variability of the surface ocean carbon cycle: A synthesis. *Global Biogeochemical Cycles*.

[Rödenbeck et al., 2022] Rödenbeck, C., DeVries, T., Hauck, J., Quéré, C. L., & Keeling, R. F. (2022). Data-based estimates of interannual sea–air CO2 flux variations 1957–2020 and their relation to environmental drivers. *Biogeosciences*, 19(10), 2627–2652.

[Schwinger et al., 2016] Schwinger, J., Goris, N., Tjiputra, J. F., Kriest, I., Bentsen, M., Bethke, I., Ilicak, M., Assmann, K. M., & Heinze, C. (2016). Evaluation of noresm-oc (versions 1 and 1.2), the ocean carbon-cycle stand-alone configuration of the norwegian earth system model (noresm1). *Geosci. Model Dev.*, 9, 2589–2622.

[Séférian et al., 2019] Séférian, R., Nabat, P., Michou, M., Saint-Martin, D., Voldoire, A., Colin, J., Decharme, B., Delire, C., Berthet, S., Chevallier, M., Sénési, S., Franchisteguy, L., Vial, J., Mallet, M., Joetzjer, E., Geoffroy, O., Guérémy, J.-F., Moine, M.-P., Msadek, R., Ribes, A., Rocher, M., Roehrig, R., Salas-y Mélia, D., Sanchez, E., Terray, L., Valcke, S., Waldman, R., Aumont, O., Bopp, L., Deshayes, J., Éthé, C., & Madec, G. (2019). Evaluation of CNRM Earth System Model, CNRM-ESM2-1: Role of Earth System Processes in Present-Day and Future Climate. *Journal of Advances in Modeling Earth Systems*, 11(12), 4182–4227.

[Takahashi et al., 1993] Takahashi, T., Olafsson, J., Goddard, J. G., Chipman, D. W., & Sutherland, S. C. (1993). Seasonal variation of CO_2 and nutrients in the high-latitude surface oceans: A comparative study. *Global Biogeochemical Cycles*, 7(4), 843–878.

[Takahashi et al., 2019] Takahashi, T., Sutherland, S. C., & Kozyr, A. (2019). *LDEO Database (Version 2019): Global Ocean Surface Water Partial Pressure of CO2 Database: Measurements Performed During 1957-2019 (NCEI Accession 0160492).* Technical report, NOAA National Centers for Environmental Information.

[Terhaar et al., 2024] Terhaar, J., Goris, N., Müller, J. D., DeVries, T., Gruber, N., Hauck, J., Perez, F. F., & Séférian, R. (2024). Assessment of Global Ocean Biogeochemistry Models for Ocean Carbon Sink Estimates in RECCAP2 and Recommendations for Future Studies. *Journal of Advances in Modeling Earth Systems*, 16(3).

[Tsujino et al., 2024] Tsujino, H., Nakano, H., Sakamoto, K., Urakawa, L. S., Toyama, K., Kosugi, N., Kitamura, Y., Ishii, M., Nishikawa, S., Nishikawa, H., Sugiyama, T., & Ishikawa, Y. (2024). Impact of increased horizontal resolution of an ocean model on carbon circulation in the north pacific ocean. *Journal of Advances in Modeling Earth Systems*, 16(2), e2023MS003720.

[Wang et al., 2022] Wang, G., Cai, W., Santoso, A., Wu, L., Fyfe, J. C., Yeh, S.-W., Ng, B., Yang, K., & McPhaden, M. J. (2022). Future southern ocean warming linked to projected enso variability. *Nature Climate Change*, 12(7), 649–654.

[Watson et al., 2020] Watson, A. J., Schuster, U., Shutler, J. D., Holding, T., Ashton, I. G. C., Landschützer, P., Woolf, D. K., & Goddijn-Murphy, L. (2020). Revised estimates of ocean-atmosphere CO2 flux are consistent with ocean carbon inventory. *Nature Communications*, (pp. 1 – 6).

[Wright et al., 2021] Wright, R. M., Le Quéré, C., Buitenhuis, E., Pitois, S., & Gibbons, M. J. (2021). Role of jellyfish in the plankton ecosystem revealed using a global ocean biogeochemical model. *Biogeosciences*, 18, 1291–1320.

[Zhou et al., 2024] Zhou, M., Tyka, M. D., Ho, D. T., Yankovsky, E., Bachman, S., Nicholas, T., Karspeck, A. R., & Long, M. C. (2024). Mapping the global variation in the efficiency of ocean alkalinity enhancement for carbon dioxide removal. *Nature Climate Change*.

Supplementary Material

S.1 Product and GOBM max/min

The full spread of fCO_2 in GOBMs and products are shown for one boreal winter and one boreal summer month in Figure S1.

S.2 Data selection for additional comparison to GOBMs

The SOCAT database for surface ocean fCO_2 [Bakker et al., 2016] is used to train the observation-based products, so cannot be used to assess their fidelity. However, these data are not used in the GOBMs, and thus can be used as an additional point of comparison.

For these comparisons, we add SOCAT data to the GLODAP+LDEOnoSOCAT dataset compiled in section 2.2. This includes averaging all data for any 1^ox1^o monthly points where data are available for more than one of the input datasets.

There are 285,256 points in the merged surface ocean global dataset "GLODAP+LDEO+SOCAT" for the period 2000-2023. This dataset is 23 times larger than the GLODAP+LDEOnoSOCAT surface ocean dataset (N=12,590, global).

S.3 GOBM comparisons to GLODAP+LDEO+SOCAT

In Figures S2 and S3, GOBMs are compared against against both GLODAP+LDEOnoSOCAT (as shown in Figure 4 and 5) and to GLODAP+LDEO+SOCAT.

Compared to GLODAP+LDEOnoSOCAT, ensemble mean bias against GLODAP+LDEO+SOCAT is 11 μatm lower in the N.SS and 2μatm higher in S.STPS and SO. In 4 of the superbiomes, the sign of the mean bias is positive for both datasets, while for the equatorial biomes, there is a slightly positive mean bias against GLODAP+LDEOnoSOCAT and a slightly negative mean bias against GLODAP+LDEO+SOCAT (-2μatm). There is a wide spread across the individual GOBM bias for both datasets.

Against GLODAP+LDEO+SOCAT, the full and seasonal timeseries, the GOBMs have lower mean uRMSE by 10 to 15μatm and higher mean correlation (r) in all superbiomes (Figure S3 and Table 2). For the variability, mean uRMSEs are slightly higher and mean correlations are higher compared to GLODAP+LDEO+SOCAT. Though improved, mean correlations for the variability remain less than 0.4 in all superbiomes.

The relative performance of different GOBMs in the ensemble is generally consistent across the two comparison datasets, indicating that the choice of dataset does not play a substantial role in assessment of relative skill compared to the ensemble mean.

GOBM performance is qualitatively consistent between the two datasets, indicating that the choice of dataset does not fundamentally change the conclusions made here. Quantitative comparisons differ somewhat. As the GLODAP+LDEO+SOCAT dataset is much larger by more than an order of magnitude, it should be better representative of the real ocean, and thus comparisons to this dataset should give a better estimate of the the true error in GOBMs. The comparisons in Figure 4 and 5 to the same independent allow assessment of the relative skill of the GOBMs and observation-based products. Since the products perform relatively better than the GOBMs when both are compared to GLODAP+LDEOnoSOCAT, and the GOBMs peform better when compared to the much larger GLODAP+LDEO+SOCAT dataset, it is possible that product performance would be assessed to be somewhat better if a much larger independent dataset were available to which they could be compared.

S.4 Data Assimilation Models

Models that use data assimilation include ECCO-Darwin [Carroll et al., 2020, Carroll et al., 2022] and ASTE-BGC [Moseley et al., 2026]. These models assimilate GLODAP and SOCAT data, so the data to which we compare in this paper are not formally independent. Nonetheless, we compare GLODAP+LDEO+SOCAT to ECCO-Darwin and ASTE-BGC to evaluate if there is evidence that current biogeochemical models with data assimilation could substantially improve the comparisons presented herein.

ECCO-Darwin is a global model available for 1992-2022 [Carroll et al., 2020, Carroll et al., 2022]. Compared to the full GLODAP+LDEO+SOCAT data in the Northern Seasonally Stratified (N.SS) superbiome for 2000-2002, we find a uRMSE of 46 μatm compared to the GOBM ensemble mean of 42 μatm and a bias of 7.7 μatm compared to the GOBM ensemble mean of 2.3 μatm. As another example, in the equatorial biome (Eq), we find uRMSE of 30 μatm for ECCO-Darwin compared to the GOBM ensemble mean of 3 μatm and a bias of -6.0 μatm compared to the GOBM ensemble mean of -2.6 μatm.

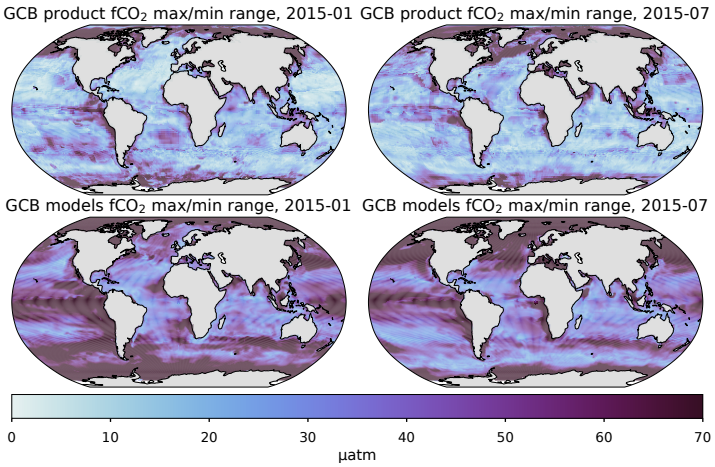

Figure S1. As Figure 1, but here with max/min spread (a) Product max/min fCO_2, January 2015, (b) Product max/min fCO_2, July 2015, (c) GOBM max/min fCO_2, January 2015, (d) GOBM max/min fCO_2, July 2015.

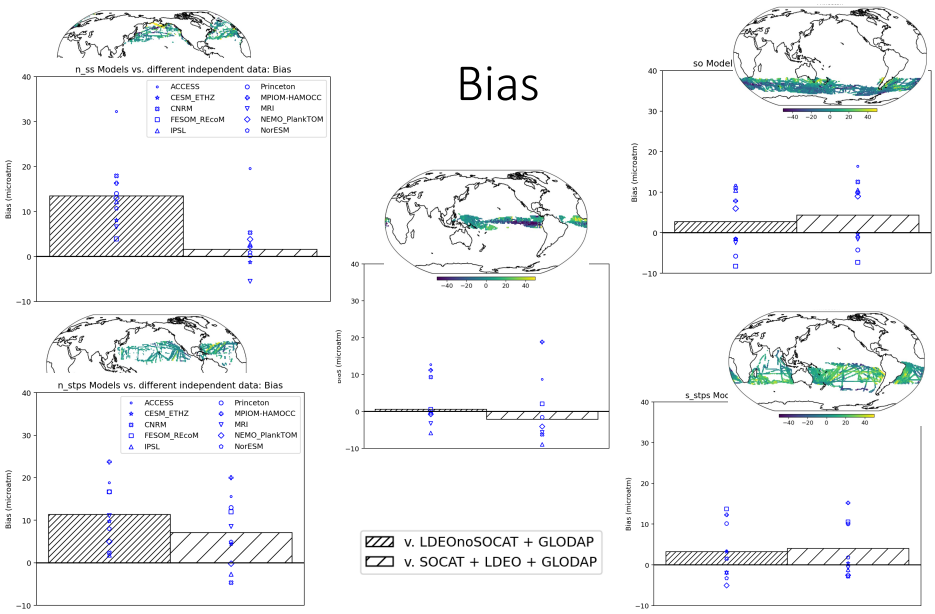

Figure S2. Bias for GOBMs against GLODAP+LDEOnoSOCAT independent data and the alternative set, GLODAP+LDEO+SOCAT. The inset maps here are for GLODAP+LDEOnoSOCAT.

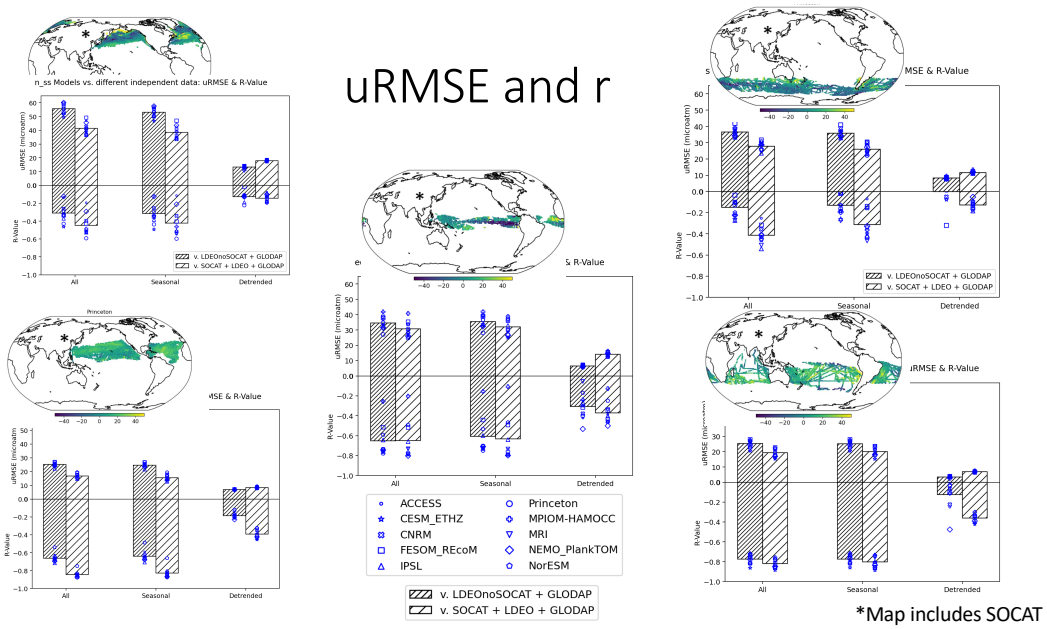

Figure S3. uRMSE and correlation for GOBMs against GLODAP+LDEOnoSOCAT independent data and the alternative set, GLODAP+LDEO+SOCAT. In each subpanel, the first set of bars is for the full dataset (All), the second for the seasonality, and the third for the remaining variability (Section 2.3 and Figure 1). The top half of each panel shows uRMSE and the bottom shows correlation. If the ensemble-mean correlation is negative, no bar is shown. The inset maps here are for GLODAP+LDEO+SOCAT to visualize its increased density in comparison to the inset maps in Figure S2.

ASTE-BGC is a regional model for the Atlantic and Arctic for the period 2002-2017 [Moseley et al., 2026]. Compared to the GLODAP+LDEO+SOCAT data for the union of the 3 North Atlantic superbiomes (excluding the North Atlantic ICE biome) [Fay & McKinley, 2014], we find a uRMSE of 35 μatm compared to the GOBM ensemble mean of 35 μatm and a bias of 9.1 μatm compared to the GOBM ensemble mean of 4.1 μatm. Detrended correlations to the data are 0.54 for ASTE-BGC and 0.52 for the GOBM ensemble mean, and seasonality is the dominant timescale.

These comparisons are not substantively different from what we have found for the GOBMs (Figures 5, S2, S3). We conclude that currently-available data assimilation models do not offer substantial skill improvements relative to the GOBMs against GLODAP+LDEO+SOCAT.

S.5 Biome to timeseries climatology comparison

Timeseries from sparse data across large open-ocean superbiomes are aggregated in this study to form the basis for comparison to products and models. This approach is justified by the common physical-biogeochemical states of these regions [Fay & McKinley, 2014] and has been widely applied [Fay & McKinley, 2021, Rodgers et al., 2023, Terhaar et al., 2024, Müller et al., 2025]. Nonetheless, particularly when applied to sparse data, aggregation has the potential to interweave signals that are strictly temporal and signals that come from heterogeneous spatial sampling. This issue does not impact biome-scale estimation of bias, uRMSE and correlation for the full timeseries ('All'), but does have potential to impact interpretation of the relative importance of time-varying seasonal mechanisms vs. variability at higher or lower temporal frequencies as the driver of underlying model or product errors.

In this section, we investigate this issue by comparing results from the Northern Subtropical Permanently Stratified (N.STPS) biome to fCO_2 climatologies at the Bermuda Atlantic Time-series Study (BATS) near Bermuda in the subtropical Atlantic [Bates et al., 2014b] and the Hawai'i Ocean Time-series (HOT) near Hawai'i in the subtropical Pacific [Karl & Church, 2014]. Data were retrieved in June 2024 from BCO-DMO and cover October 7, 1991 to June 22, 2023 for BATS and October 31, 1988 to September 1, 2022 for HOT. Data were averaged to monthly resolution, and then detrended and climatologically averaged as explained in Section 2.3. Product and model estimates from the gridcell closest to BATS (31.8N, 64.2W) and HOT (22.8N,158.0W) were extracted and processed in the same way.

In Figure S4, the N.STPS, BATS and HOT climatologies are compared. The N.STPS climatology lies between the larger-amplitude BATS and smaller-amplitude HOT climatology. For all three comparisons, the products (left column) are consistently closer to the observations than the models (right column). In Figure S5, product and model bias, uRMSE and correlation for N.STPS, BATS and HOT are presented. Bias (left column) is under $\pm 5\mu$atm for the products, and ranges from -3 to $+17\mu$atm for the models. Bias estimates differ across the full N.STPS superbiome, and BATS and HOT gridcells, indicating that there is substantial spatial compensation occurring in biome-mean bias estimates, as expected from prior research [Gloege et al., 2021, Müller et al., 2025]. A consistent finding across N.STPS, BATS and HOT is larger bias and a larger spread of bias across the model ensemble, compared to the product ensemble. The ordering of bias in individual models relative to the ensemble mean is generally consistent across N.STPS, BATS and HOT.

In N.STPS, the mean uRMSE for the full timeseries comparison is 21μatm and 25μatm for the products and models, respectively. At the timeseries sites, these values are smaller, 14μatm and 16μatm, respectively at BATS and 8.5μatm and 8.3μatm, respectively at HOT. Correlations are lower ($\sim$0.7) for N. STPS and $>$0.9 for BATS and HOT. These results are comparable to that reported in Gloege et al. (2022). The decomposed seasonality causes a smaller portion of the total uRMSE at BATS and HOT than for N. STPS, but in all cases, drives most of the correlation. For the non-seasonal variability, all three datasets have modest uRMSE (6-12μatm) and low correlation. Interestingly, variability in the models is more highly correlated at BATS and HOT than N. STPS, while correlations are similar for the products. This suggests that an inability to capture spatial patterns of variability may play a more prominent role in the models. Overall, these findings are consistent with the conclusion from the main text that non-seasonal variability is poorly correlated with independent observations in both products and models.

In summary, these results suggest that approximately half of the seasonal uRMSE found in the biome-aggregated N. STPS timeseries may be due to temporal mismatch of seasonal behavior in the products and models, with the remainder due to the heterogeneity of spatial sampling that projects onto the aggregated timeseries. Better quantifying this and determining the extent to which these findings hold for the other biomes would require additional long-term monthly

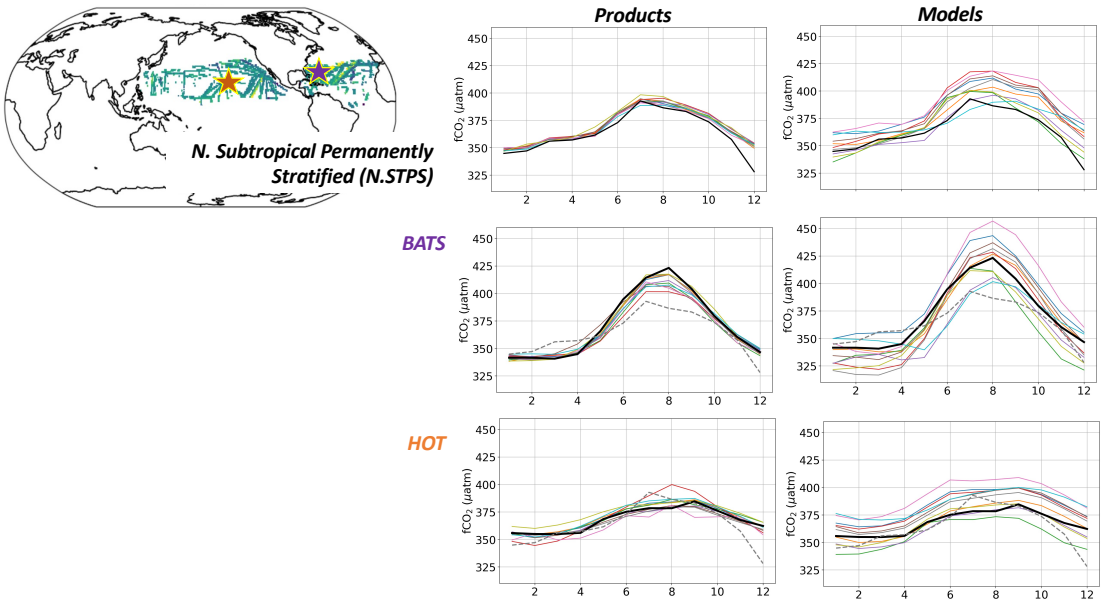

Figure S4. Comparison of N.STPS biome climatology to the climatology of fCO_2 from two northern hemisphere subtropical timeseries, for products (left column), models (right column). In the panels for BATS and HOT, the grey dashed line is the Northern Subtropical Permanently Stratified (N.STPS) biome climatology from the top row, to aim in visual comparison. The inset map indicates the data in GLODAP+LDEOnoSOCAT for N. STPS, the Bermuda Atlantic Time-series Study (BATS) near Bermuda in the subtropical Atlantic (purple star) and the Hawai'i Ocean Time-series (HOT) near Hawai'i in the subtropical Pacific (orange star).

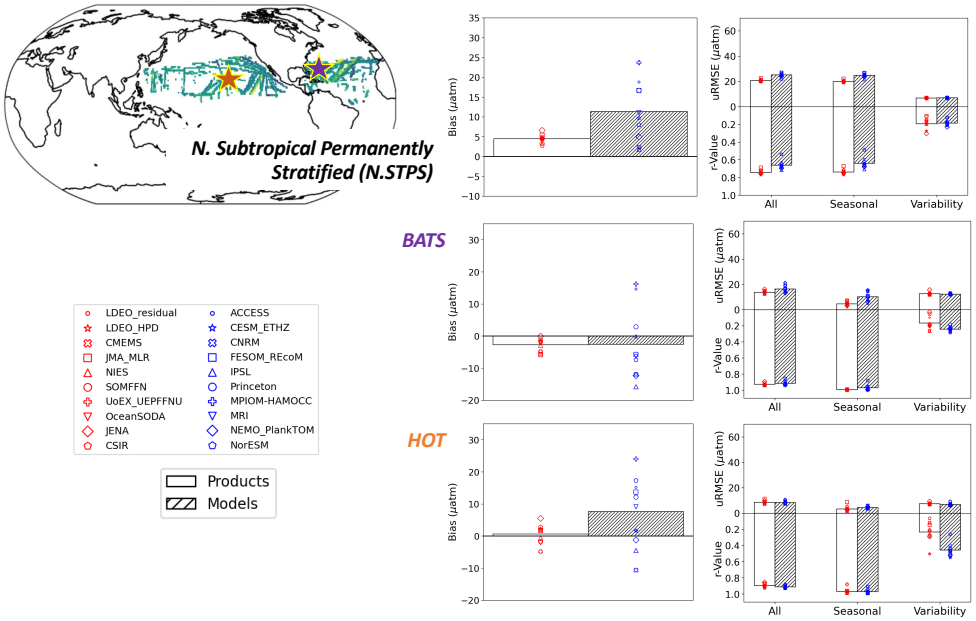

Figure S5. Comparison of N.STPS biome bias (left column), uRMSE and correlation (right column) to BATS and HOT.

timeseries data, which unfortunately are not readily available [Bates et al., 2014a].